

# First-principles simulations of dislocation cores

C. Woodward<sup>a,b</sup>

<sup>a</sup> Materials and Manufacturing Directorate, Air Force Research Laboratory, AFRL/MLLM, Wright-Patterson AFB, OH 45433-1894, USA

<sup>b</sup> Department of Materials Science and Engineering, Northwestern University, Evanston, IL 60208-3108, USA

Received 8 October 2004; received in revised form 28 January 2005; accepted 28 March 2005

## Abstract

In order to understand the “chemistry of deformation” an adequate description of the strain field near the center of dislocations (the core) is required. We review the development and current status of ab initio methods that have been used to model the core structures of dislocation in elemental refractory metals and intermetallic alloys. Methods employing flexible boundary conditions or dislocation dipoles allow for the direct simulation of dislocations while methods based on the Peierls–Nabarro approximation use the generalized stacking-fault energy to model the restoring force across the lattice discontinuity produced by the dislocation. This energy function can be derived from first-principles reference calculations. In this work we emphasize methods and their application to materials where plastic deformation is complex and Schmid's law is violated.

© 2005 Elsevier B.V. All rights reserved.

**Keywords:** Dislocations; Dislocation cores; First-principles methods; Refractory metals; Intermetallics

## 1. Introduction

Many materials properties which are critical for structural metals are directly related to the production, mobility and evolution of dislocations. Plastic deformation is controlled by the interaction of dislocations with the host lattice, the applied stress, and with other defects such as other dislocations, solutes, grain boundaries and precipitates. Continuum elasticity methods have been very successful in describing the long-range stress fields of dislocations. The utility of these methods is illustrated in the recent progress shown in the dislocation dynamics community in describing the time evolution of large numbers ( $>10^6$ ) dislocation segments. However, atomistic methods have shown that the forces produced at the center of the dislocation (the core region) and their coupling to the applied stress can have a dramatic effect on plasticity. Of particular interest are applications to refractory bcc metals and high temperature intermetallics where Schmid's law is generally violated. These materials also exhibit a large lattice friction stress at low temperature, and a decreasing lattice friction stress with increasing temperature

up to approximately 20% of the melting temperature for the bcc metals. Deformation is often dominated by straight screw dislocations, implying that these dislocations experience the largest lattice friction stress. For more details on the complex deformation behavior of the bcc metals several excellent reviews are available [1,2]. Current consensus is that this complex flow behavior is produced by dislocation cores that are spread in more than one glide plane. Continuum methods are unable to describe this short range interaction as the method diverges in the core region. While atomistic methods have merit in describing trends in materials behavior they are limited by the fidelity of the assumed interaction model and for this reason are at best semi-empirical. Several methods, based on first-principles calculations, have emerged in the last few years for modeling dislocations in metals. Currently available, large scale electronic structure methods are based on a super-cell method, where periodic symmetry is enforced along the three lattice directions. Modeling an isolated dislocation using these methods is problematic for several reasons. First, the stress field produced by an edge or screw dislocation is proportional to the inverse of the distance to the dislocation center. In conventional atomistic methods a surface is used to accommodate the discontinuity in the lattice produced by

E-mail address: christopher.woodward@wpafb.af.mil.

the Burgers vector, and a large buffer region ( $\sim 10^4$  atoms) is used to isolate the dislocation core from the surrounding static lattice. Simulation cells of this size are beyond the scope of current electronic structure methods. Second, the geometry of an isolated dislocation breaks periodic symmetry in the plane normal to the dislocation line direction which is inconsistent with the underlying boundary conditions imposed by the super-cell methods.

Several approaches have been developed to circumvent these boundary condition issues. These techniques can be divided into three classes: (i) simulation of dislocation dipoles arrays, (ii) direct simulation of isolated dislocations using flexible boundary conditions and (iii) a two-dimensional Peierls–Nabarro description of the core based on the generalized stacking fault derived from first-principles reference calculations. In the next section we will describe the approximations and limitations of each of these methods. We will then review recent results obtained from these techniques and compare the merits of each approach.

## 2. First-principles methods

### 2.1. Simulation of dislocation dipoles

The symmetry of a single dislocation is incompatible with periodic boundary conditions. The cut in the lattice, introduced to produce the dislocation, makes it impossible to match the lattice normal to the dislocation line without introducing a large artificial stress field. Dislocations in Si have been treated for some time using a periodic arrangement of dislocation dipoles [3]. In these simulations the dipoles are arranged such that the superposition of the elastic stress fields produces zero stress at any dislocation center. Studies of dislocations in Si uncovered many of the issues that need to be addressed when using this technique. For example, some care must be taken when developing the periodic cell in order to avoid forming parallel tilt boundaries [3]. Initial applications produced incompatibility stresses due to improper arrangements of the dislocation dipoles [4]. These issues were resolved for dislocation in Si in later publications [5]. Also, Cai has recently pointed out that elastic anisotropy can effect the results of these calculations, and offers a procedure to minimize the error of such techniques [6].

In the bcc metals initial applications of this technique focused on the  $a/2(1\ 1\ 1)$  screw dislocations in Mo and Ta [7]. Here dislocations of opposite burgers vectors were placed in a quadra-pole arrangement within a supercell calculation of 90 atoms. The distances between dislocation centers in these simulation cells were less than  $3.3b$  ( $8.8\text{ \AA}$ ). Two initial configurations were considered, the so-called hard mode and the soft mode dislocation sites. The hard core occurs when the anisotropic displacement field for the dislocation shifts the local arrangement of atoms such that they lie in the same  $(1\ 1\ 1)$  plane. Earlier Duesbury had proposed that this high

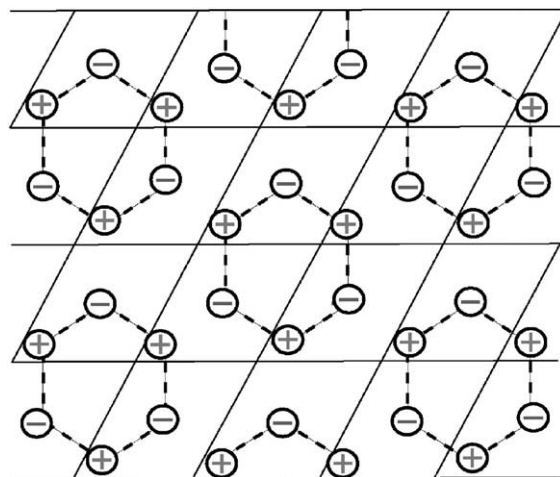


Fig. 1. A schematic of the hexagonal array of dislocations used to model dislocations in Fe and Mo after the work of Frederiksen and Jacobsen [8]. Cells outlined by lines are the periodic cell used to model the dislocation dipoles. The position of the dislocations are shown as circles centered on '+' and '-' symbols representing the positive and negative burgers vectors.

energy configuration may be sampled by a dislocation gliding between soft mode sites. The ensemble was optimized using a pseudo-potential plane wave method.

More recently, Frederiksen and Jacobsen examined the equilibrium dislocation cores in bcc Fe and Mo using a plane wave pseudo-potential method and dislocation dipoles [8]. In this case the dislocation dipoles were arranged to form a hexagonal grid, which is commensurate with the projected  $(1\ 1\ 1)$  plane in the bcc lattice (Fig. 1). In these calculations the distance between dislocation centers is between  $4.4b$  ( $11.7\text{ \AA}$ ) and  $5.4b$  ( $14.6\text{ \AA}$ ). These simulation cells allow the dislocation cores to be placed exactly centered between three columns of atoms in the screw direction, which is the expected equilibrium configuration. Also, the dislocation cores are separated by more than  $4b$ , which is greater than expected extent of the individual dislocation cores as found using atomistic methods [9].

### 2.2. Simulating isolated dislocations using flexible boundary methods

We have developed an ab initio flexible boundary condition method based on a lattice Greens function (LGF) which is derived from simple first-principles reference calculations. The lattice Greens function can be derived directly using a simple numerical procedure describe in the literature [10,11] or by deriving the dynamical matrix using a direct force method or a first-principles linear response calculation [12]. In our studies we have applied the ab initio total-energy and molecular dynamics program, the Vienna ab initio simulation package (VASP), which was developed at the Institut für Theoretische Physik, Technische Universität Wien [13]. However, any electronic structure method that produces reliable Hellmann–Feynman forces could be employed. Details

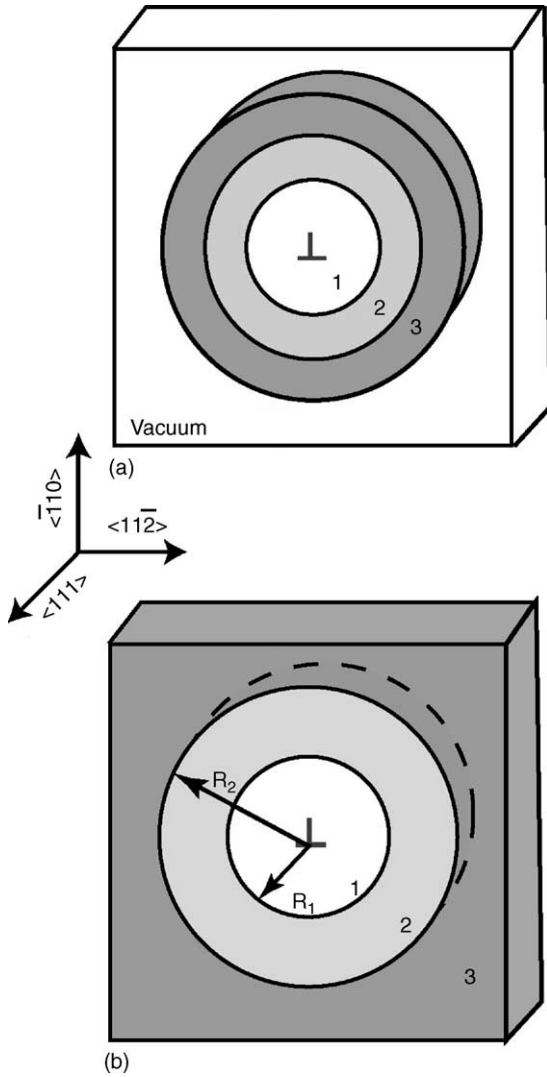


Fig. 2. Schematic diagrams of the two types of simulations cells used to model dislocations in the FP-LGFBC method. In (a) a vacuum region is used to terminate the dislocation and (b) a domain boundary is employed.

of the calculations for  $a/2(1\ 1\ 1)$  screw dislocations in bcc Mo and Ta and  $a/2(1\ 1\ 0)$  screw dislocations in  $L1_0$  TiAl can be found in the literature [14–16].

The strain field of the dislocation core is contained using the two-dimensional lattice Greens function. We have employed two different types of simulation cells, one consistent with traditional atomistic simulations where the active region is terminated with a vacuum region (Fig. 2a) and a new approach where the simulation cell is terminated at a domain boundary (Fig. 2b). The dislocation is placed within two concentric cylindrical regions where region three is used to isolate the dislocation core from the vacuum region, or the domain boundary formed at the edge of the simulation cell [14,15]. The vacuum region present in the traditional simulation cell introduces inefficiencies during the simulation. By design the plane wave basis represents the electron density using a uniform fast fourier transform grid and this representation in the vacuum region is very inefficient. The compu-

tational effort of the electronic structure method scales with the cell size and the solution in the vacuum region is not our primary focus. Also, during optimization the electrons will form a charge dipole across at the metal surface and produce image forces in region 3. We find that simulation cells using a domain boundary are numerically more efficient as the perturbation in the charge density is smaller at the boundary and cell sizes are significantly reduced. Also we find that both cells converge to the same result at reasonable cell sizes. The relaxation procedure for these cells proceeds as follows. An initial atomic displacement field, from anisotropic elasticity theory is applied to a cell such as those shown in Fig. 2. Region 1 is then relaxed using the Hellmann Feynman forces from the first-principles calculation. Incompatibility forces, generated for atoms in region 2, are removed by displacing all the atoms within the simulation cell according to the Greens function (GF) solution:

$$u_i^m = \sum_{j,n} G_{ij}^{mn}(R_{mn}) f_j^n \quad (1)$$

where the indices  $m, n$  denote atoms, the indices  $i, j$  denote the Cartesian components,  $R_{mn} = R_n - R_m$  and  $f_j^n$  are the Hellmann–Feynman forces. This process is repeated until the atomic forces in regions 1 and 2 are converged. The iterative process is required because region 1 contains a defect and the LGF is consistent with the bulk crystal. Also, the LGF is only required for only short range (less than  $\sim 5$  Å) interactions, for longer range interactions the LGF converges to the elastic Greens function. Thus for interactions between atoms where  $R_{mn}$  is larger than 5 Å we employ the elastic Greens function. The required elastic GF is generated from the reference calculations of the elastic constants. Finally, in the first-principles adaptation of the GFBC all the atoms are moved according to the derived Hellmann–Feynman forces at all steps of the optimization procedure.

The FP-GFBC method is also uniquely suited for estimating the Peierls stress. Typically a binary search over the applied stress is used to determine the smallest stress needed to move the dislocation one periodic unit. In conventional fixed-boundary methods, as the dislocation moves it converts elastic strain into work. For small cells this can be a very large effect, in some cases all the applied stress can easily be converted into work as the dislocation glides. The problem is most apparent in materials with a large Peierls stress. Therefore it is difficult, if not impossible, to estimate the lattice friction stress using fixed boundary conditions in a small atomistic region. The flexible boundary condition method restores the applied stress at each update of the GFBC. The largest applied stress under which the dislocation does not move a periodic distance is a lower bound to the Peierls stress. Several groups have developed constant stress simulations, where the stress is automatically maintained at a certain level by monitoring the stress tensor of the simulation cell. This technique will be limited by the size of the update step used in the optimization procedure.

### 2.3. Generalized stacking fault methods

The concept of a generalized stacking fault was introduced in the 1960's by Vitek in the context of exploring the possibility of stacking faults in the bcc metals [17] using atomistic potentials. In the original formulation this representation was called a “ $\gamma$  surface”. The atomistic interaction energy across a shear plane is derived by displacing the two half crystals an infinitesimal amount in that plane while allowing atoms to relax normal to the shear plane. The process is then repeated until the energy surface of the entire two-dimensional periodic cell is generated. The original derivation of  $\gamma$  surfaces were based on atomistic potentials, however, in the early 1990's several groups began to derive parts or all of the  $\gamma$  surfaces using ab initio methods [18–20]. Taking the negative of the gradient of the energy as a function of the displacement vector yields a restoring force, or stress, across the plane of the cut.

In the original Peierls Nabarro model the core structure of a dislocation is derived by balancing the forces produced by deforming two half crystals with a one-dimensional periodic potential acting across the glide plane [21,22]. The model is attractive in its simplicity, incorporating atomistic effects into a continuum framework. However, it involves solving an integral equation:

$$C \int_{-\infty}^{\infty} \frac{p(x')}{x - x'} dx' = F(u), \quad p(x) = \frac{du}{dx} \quad (2)$$

where  $p(x)$  is subject to a normalization condition corresponding to the closure failure produced by the burgers vector. Here  $x$  is in the plane of the dislocation core perpendicular to the line direction, and  $u(x)$  is the misfit in the direction of the burgers vector. Eq. (2) equates the restoring stress of the atoms interacting across the glide plane,  $F(u)$ , with the stress produced by a continuous distribution of infinitesimal dislocations ( $p(x)$ ). The analytic solution for the PN model for a sinusoidal potential takes a  $\tan^{-1}$  form, though in practice the potential realized in an actual lattice may be more complex. As pointed out by Christian and Vitek the stress relation,  $F(u)$ , can be approximated by the gradient of the generalized stacking energy [23].

The simple one-dimensional PN model has been extended to treat more complex two-dimensional geometries by Schoeck [24]. This was accomplished by introducing a flexible representation of the displacement potential based on a two-dimensional Fourier series. A variational procedure is used to minimize the energy by optimizing the fourier coefficients describing the displacements in the glide plane. This representation of balance in energy between the two elastic half crystals and the misfit potential across the plane of the glide plane now contains optimized relaxations in the glide plane. This relationship is expressed as a system of integro-differential equations:

$$\frac{K_{\alpha\beta}}{2\pi} \int_{-\infty}^{\infty} \frac{d\xi}{\xi - x} \frac{du_{\beta}}{d\xi} = F_{\alpha}(\bar{u}) \quad (3)$$

where the subscript  $\beta$  refers to the components of the displacements  $\bar{u}$  ( $\beta=1$  for screw,  $\beta=2$  for edge), and  $K_{\alpha\beta}$  is equal to  $\mu\delta_{\alpha 1}$  and  $\mu\delta_{\alpha 2}/(1 - \nu)$  for  $\beta$  equal to 1 and 2, respectively. Employing the generalized stacking fault energy the local restoring force can be defined as  $F_{\beta}(u) = -dE(\bar{u})/du_{\beta}$ , where  $E(\bar{u})$  can be defined parametrically or derived using atomistic or ab initio calculations. Mryasov and co-workers have used this approach to study the core splitting of ordinary and super-dislocations in several intermetallics [25]. Here a more general solution to Eq. (2) is proposed where a general analytic complex function is used to evaluate the dislocation density in combination with first-principles GSF calculations.

Ngan has developed a generalization of this method which can be applied to dislocation cores that are non-planar (e.g. the core spreads onto more than one glide plane), for example screw dislocations in the bcc metals [26]. This is based on a conformal mapping of the slip plane onto several glide planes which intersect along a common line. Following Ngan, when a screw dislocation spreads symmetrically over  $2n$  identical planes the PN equations can be modified:

$$\frac{4n\mu x^{2n-1}}{\pi} \int_0^{\infty} \frac{d\xi}{\xi^{2n} - x^{2n}} \frac{du_{\beta}}{d\xi} = F_{\alpha}(\bar{u}) \quad (4)$$

where  $u$  and  $F$  are the displacements and the misfit force law across each of the identical  $2n$  slip planes. Ngan has used a

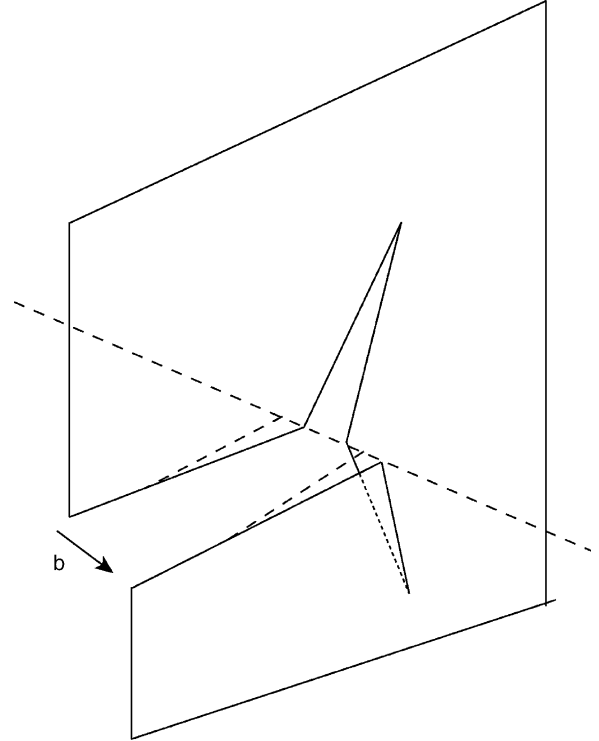


Fig. 3. Schematic of the screw dislocation in the bcc transition metals using the GSF model as suggested by Ngan [26]. Here the dislocation is divided into three partials spread on (1 1 0) planes around the dislocation line. The original (1 1 1) plane normal to the line direction is shown with the cut and displacement along (1 1 1) needed to form the screw geometry.



Raleigh-Ritz procedure to produce an approximate solution to Eq. (4) and explored analytical solutions by deriving an inverse transform to Eq. (4) and solving the resulting boundary value problems [26]. Fig. 3 shows a schematic of the bcc screw dislocation envisaged by Ngan. The core is assumed to take on a strongly anisotropic distribution of strain, spreading asymmetrically on three (1 1 0) planes.

Another modification of the PN model, distinct from the work of Schoeck, was proposed by Bulatov and Kaxiras in order to treat very narrow dislocation cores (e.g. Si) [27]. This semidiscrete-variational Peierls framework includes the discrete nature of the underlying lattice and the information contained in the GSF in a variational procedure for optimizing the PN integro-differential equations. They also develop a technique for evaluating the Peierls stress within this variational method which appears to give better estimates of the Peierls stress for Si compared to previous methods. This technique was also used to study the ordinary dislocation in Al with and without H solid solutions by introducing an energy functional that includes elastic, misfit and stress terms [28].

### 3. Results and discussion

#### 3.1. Elemental bcc metals

In their dislocation dipole study Ismail and Arias focused on the energy difference between the soft and hard cores in the bcc transition metals Mo and Ta. Based on the energy landscape, estimated from the energy difference between these two states, they suggested that the Peierls stress of straight screw dislocations was significantly smaller than that expected from classical theory and atomistic simulations [7]. Also, they found that the equilibrium dislocation cores for Mo and Ta spread symmetrically about a central point on the (1 1 0) planes (e.g. symmetric cores). Using the FP-GFBC method Woodward and Rao calculated the equilibrium geometry for screw dislocations in bcc Mo and Ta and confirmed that the dislocation cores for Mo and Ta are spread evenly about a central point on (1 1 0) planes [14]. Woodward and Rao also applied several types of pure shear stress on a periodic, straight screw dislocation and found that the primary Peierls stress is large ( $\sim 0.02 \mu\text{m}$ ), consistent with classical models of deformation in the bcc metals [14]. The core spreading for an isolated dislocation in Mo predicted using atomistic potentials and the FP-GFBC method is shown in Fig. 4a using differential displacement plots. Atomistic potentials fit to materials parameters for the group V bcc transition metals produce a core similar to that shown in Fig. 4a. However, atomistic potentials for the group VI metals (e.g. Mo) all show a distinctive asymmetric spreading of the core on the (1 1 0) planes. A representative core structure, calculated for bcc Mo using an atomistic potentials based on the model generalized pseudo-potential theory (MGPT), is shown in Fig. 4b [29]. While the differences in the core structure may seem subtle, over the last 25 years these distinctions

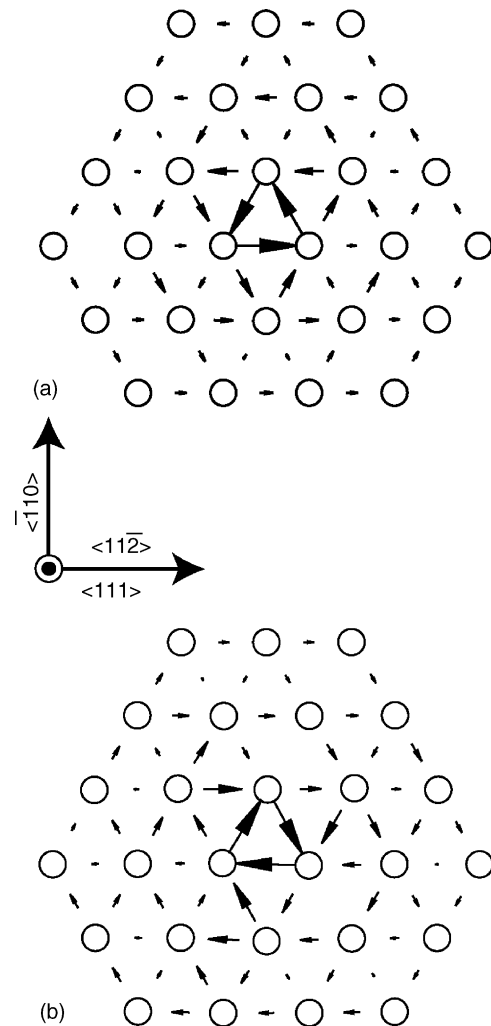


Fig. 4. Differential displacement plots of the screw component of an  $a/2(1\ 1\ 1)$  screw dislocation in Mo. Fig. 3a shows the equilibrium core found using the FP-LGFBC method and Fig. 3b shows the equilibrium core found using the LGFBC method with atomistic potentials.

have been used to explain the variation in plasticity between the group V and group VI bcc transition metals. Correlation of the variations in core structure to the sensitivity to non-glide stress is one of the main results of atomistic simulations in the bcc metals. For this reason, we have performed a series of calculations using the FP-GFBC method checking convergence with cell size and using the asymmetric displacement field produced by atomistic simulations as the starting configuration for the optimization procedure. All these calculations produced a symmetric spreading of the core (Fig. 4a) in contrast to the predictions of all previous atomistic simulations [15].

The nomenclature used to describe the equilibrium shape of these dislocation cores is derived from interpretations of differential displacement plots which are typically shown as a projection along the screw axis. In these plots the relative displacement of neighboring atoms is represented by an arrow centered between the two relevant atoms. The scale

for the screw components is such that a  $b/3$  displacement will produce an arrow with a length that spans the nearest neighbor distance between atoms in the  $(1\ 1\ 1)$  projection. Traditionally, the differential displacement plot shown in Fig. 3a is characterized as: symmetric, non-degenerate or a six-fold core. The core shown in Fig. 3b would be characterized as non-symmetric, degenerate or a three-fold core. The term symmetric versus non-symmetric refers the anisotropy in spreading of the core on the  $(1\ 1\ 0)$  planes. The term degenerate (Fig. 3b) is used to highlight the fact that this core has variant which is rotated by  $120^\circ$  about the line axis. The term six-fold core is somewhat misleading, as it implies that there is a six-fold rotation axis along the line direction. While the bcc lattice has a  $C_3$  rotation axis along  $(1\ 1\ 1)$ , the dislocation produces screw axis along  $(1\ 1\ 1)$ . In order to map the lattice back into itself each  $120^\circ$  rotation about the line axis is accompanied by a lattice translation of  $b/3$ . In the  $(1\ 1\ 1)$  projection, used to view the dislocation, we will naturally observe a  $C_3$  symmetry the implied  $D_3$  symmetry of a six-fold core is not a symmetry of the underlying lattice. It is also important to note that there is a continuous distribution of dislocation cores ranging from the two extreme cases of symmetric and non-symmetric. Duesbury found a correlation between the shape of the core and the position of the three atoms adjacent to the dislocation core [30]. The bcc lattice will allow these atoms the freedom to shift uniformly along the screw direction by a value ranging from  $-b/6 < p < b/6$ , where  $p$  is defined as the polarization of the core [31]. Anisotropic elasticity theory produces a dislocation core with  $p = 0$ , when atomic scale forces are introduced (by atomistic potentials or first-principles methods) invariably  $|p| > 0$ . Thus in the most rigorous sense all the dislocation cores modeled using atomistic forces are “degenerate”, though the energy needed to transform from one variant to the other is expected to be larger for dislocations with a large polarity. These energy barriers are most relevant in simulations of kinks, where all combinations of possible variants need to be considered [29].

We have investigated the degree of polarization of the screw dislocation in bcc Mo using the FP-GFBC method. These calculations were performed on cells of increasing size ranging from an  $R_2$  (Fig. 2b) of 12.2 to 23.3 Å (168–504 atom cells). The resulting polarization (Fig. 5) oscillates slightly ( $\sim 0.017b$ ) with increasing cell size and converges to a value of  $p \sim 0.025 (b/6)$  for cells large than  $R_2 \sim 20$  Å. Thus the polarity decreases slightly with increasing cell size, consistent with the differential displacement plots that show a “symmetric” core independent of cell size.

Up to this point in time differences in the macroscopic plasticity of the group V and VI transition metals, for example higher sensitivity to non-glide stresses propensity in the group VI metals, had been linked to the differences in the equilibrium core structures. Duesbury and Vitek found that atomistic potentials, fit to the elastic and formation energies of the bcc transition metals, produce strongly asymmetric cores for the group VI metals and symmetric cores for the group

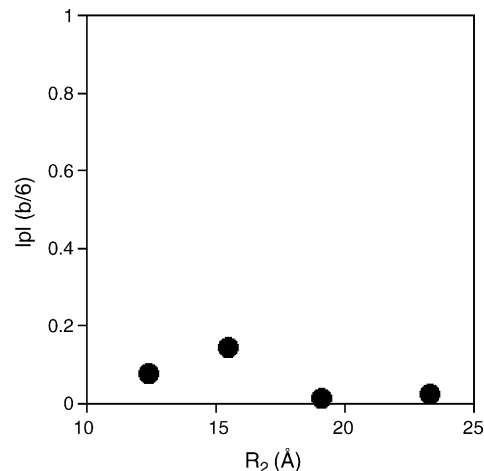


Fig. 5. The polarization of the  $a/2(1\ 1\ 1)$  screw dislocation in Mo as a function of cell size derived using the FP-GFBC method.

V metals [32]. The differences in core shape could be rationalized by studying differences in the generalized stacking fault. They found that the atomistic potentials for the group VI metals produced a  $\gamma$  surface that favored the formation of three  $b/3$  dislocations on the  $(1\ 1\ 0)$  planes ( $\gamma(b/3) < 2\gamma(b/6)$ ) while the group V metals favored the formation of six  $b/6$  dislocations ( $\gamma(b/3) > 2\gamma(b/6)$ ). A schematic of the gamma surfaces illustrating this relationship is shown in Fig. 6 [32].

We have determined the  $(1\ 1\ 1)$  cross section of the  $(1\ 1\ 0)$   $\gamma$  surface in Mo and Ta using an ab initio method (VASP). Here the  $\gamma$  surface was derived using the traditional equation of constraint for atomistic relaxations normal to the glide plane (see Section 2.3). The results, Fig. 7, are shown with energy scale normalized to the maximum value of  $\gamma$  along  $(1\ 1\ 1)$ . In this representation the energy with shear for these two materials appears almost identical. We find for both Mo and Ta that  $\gamma(b/3) > 2\gamma(b/6)$  which satisfies the condition favoring the “symmetric” core. Using an ab initio dislocation-dipole method Fredericksen and Jacobsen recently confirmed a “symmetric” dislocation core for bcc Mo [8]. Also, they predict a similar dislocation core for

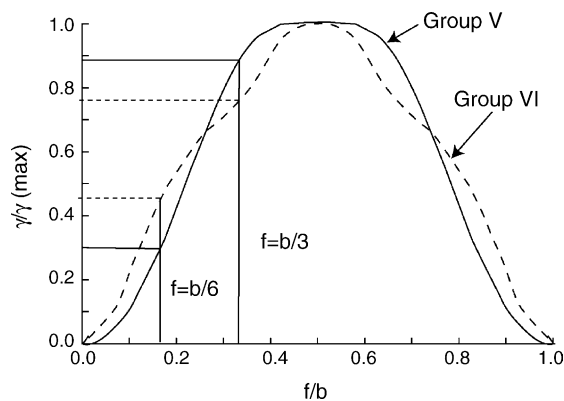


Fig. 6. Schematic of the  $(1\ 1\ 1)$  cross section of  $(1\ 1\ 0)$   $\gamma$  surface for the group V and group VI bcc transition metals found by using atomistic methods [32].

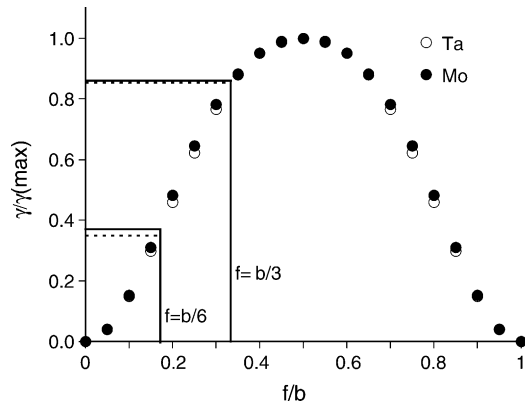


Fig. 7. First-principles (VASP) derived (1 1 1) projection of (1 1 0)  $\gamma$  surface for Mo and Ta.  $\gamma(\max)$  is equal to 0.092 and 0.047 eV/Å<sup>2</sup> for Mo and Ta respectively. The value for  $\gamma(b/6)/\gamma(\max)$  is 0.367 (0.3508) in Mo (Ta) and for  $\gamma(b/3)/\gamma(\max)$  0.853 (0.846).

ferro-magnetic Fe. Further, they generated ab initio gamma surfaces for the (1 1 0) and (1 1 2) type planes with shear in the (1 1 1) direction for all the bcc transition metals. They find for all the bcc transition metals that the condition for the symmetric core ( $\gamma(b/3) > 2\gamma(b/6)$ ) is satisfied. Recent atomistic and tight binding methods have attempted to incorporate the shape of the core derived from the first-principles methods in the construction of the atomistic interaction schemes. Atomistic models for Mo have been modified to produce a symmetric core and tight binding methods have been modified to include screening interactions in order to produce a similar result.

Before leaving the FP-GFBC results for the bcc metals it is worth noting that these screw dislocations also produce small but finite edge components in the vicinity of the dislocation core. These components interact strongly with non-glide stresses and can produce significant deviations from Schmid's law. The edge components for the  $a/2(1 1 1)$  screw dislocation in Mo and Ta are shown in Fig. 8, in this case the displacements are scaled by a factor of 10 in order to make them more visible. While the positions and direction of the edge components are different from that found using atomistic potentials the two methods cover approximately the same cross sectional area in the core region.

In principle the method of Ngan, which extends the GSF-PN model to non-planar dislocation cores, could be applied to modeling dislocation cores in the bcc metals [26]. If we represent the symmetric dislocation core as a distribution of six partial burgers vectors on the (1 1 0) planes, and the asymmetric dislocation core by three partials burgers vectors distributed on the (1 1 0) planes the formalism suggests that the latter dislocation core would have a lower energy. Also, it is not clear if the additional structure found in the gamma surfaces for atomistic potentials of the group VI bcc transition metals would produce an asymmetric dislocation core when employed in the GSF-PN model. The geometry produced by symmetric dislocation cores present serious challenges to the GSF-PN model because near the core region (i.e. a cylinder

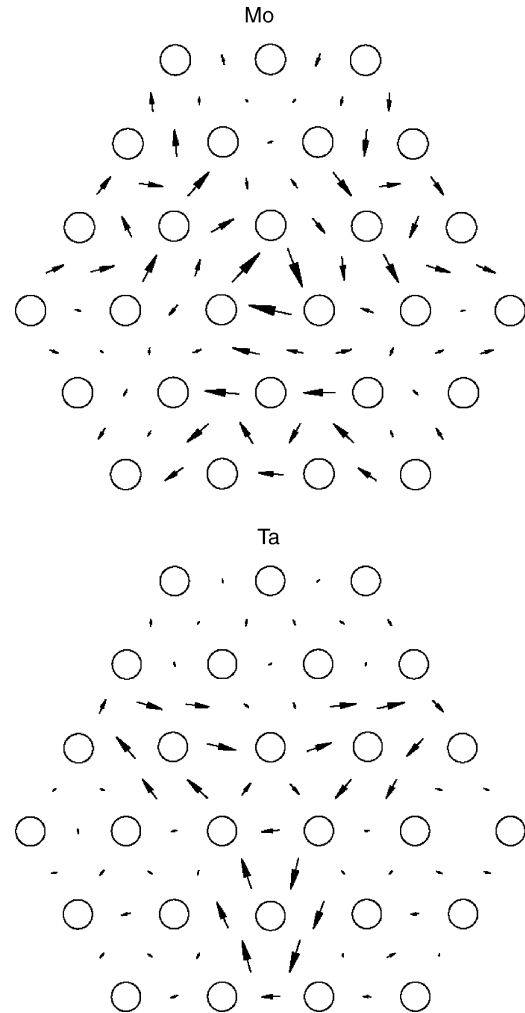


Fig. 8. Differential displacements plots of the edge displacements for an  $a/2(1 1 1)$  screw dislocation in Mo and Ta calculated using the FP-GFBC method described in the text.

of radius  $4b$ ) the linear approximation breaks down. Given the problems with elasticity theory near the core region it is unlikely that this method would produce reliable predictions for the strain field or the Peierls stress for the non-planar cores found in the bcc metals.

### 3.2. Intermetallics

There is significant interest in understanding the evolution of dislocation cores under stress in intermetallic alloys used in high temperature applications. For example we have employed the FP-GFBC method to calculate the equilibrium core structure and Peierls stress of the  $a/2(1 1 0)$  screw dislocation in  $\gamma$ -TiAl. These materials exhibit an increasing yield stress with increasing temperature and several groups have proposed that this effect is in part due to the cross slip of ordinary screw dislocations. Louchet and Viguier proposed that these cross slipped segments form pinning points by the collision of kinks running on different (1 1 1) glide planes [33] and Sriram and co-workers have proposed a double cross slip

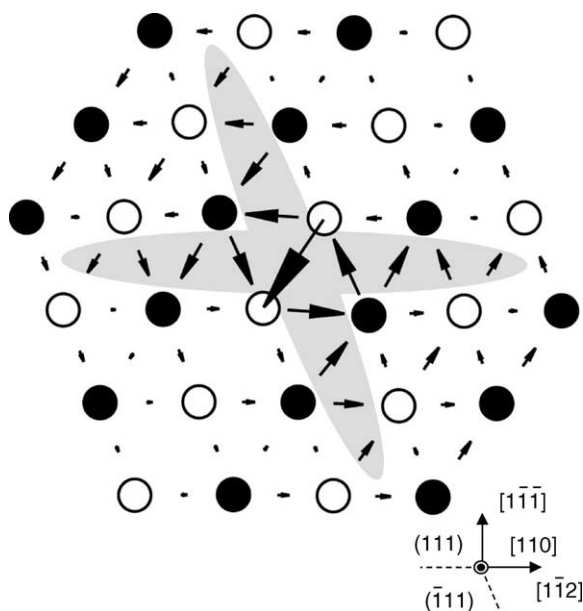


Fig. 9. Differential displacement plots of the screw component of an  $a/2(1\ 1\ 0)$  screw dislocation in  $\gamma$ -TiAl found using the FP-GFBC method [15].

process which results in a sessile jogged segment [34]. Both these mechanisms are dependent on the ready cross slip of the ordinary dislocation. From predicted (complex) stacking fault energies and after several atomistic studies it was unclear if this dislocation assumed a planar configuration dissociated into two partials separated by a complex stacking fault or if the core was better represented by the total (screw) dislocation. The latter configuration would be more amenable to cross slip. We have used the FP-LGFBC method to calculate the equilibrium core of the  $a/2(1\ 1\ 0)$  screw dislocation in TiAl, this core is shown in Fig. 9. The predicted core is spread equally on two  $(1\ 1\ 1)$  planes, a configuration which is similar in spirit to that predicted for the screw dislocations in the bcc transition metals. Previously, Mryasov and co-workers have calculated the density of displacements for the same dislocations using the GSF-PN model, using a  $\gamma$  surface derived from first-principles calculations [25]. A schematic of the results of these calculations are shown in Fig. 10 as a distribution of the density of displacements in the glide plane. Unfortunately the assumed core geometry for this GSF-PN model was a planar configuration, using the method proposed by Ngan [26] this constraint could be relaxed. However, as in the case for the bcc metals the linear approximation may break down in the region where the dislocation is spread on two planes.

Mryasov and co-workers have used the GSF-PN model extensively to model intermetallics these include simulations of  $L_{12}$  Ni<sub>3</sub>Al, Ni<sub>3</sub>Ge and Fe<sub>3</sub>Ge [25] and B2 NiAl where planar dislocation cores are expected. Also, Kohlhammer and co-workers have considered core spreading of super-dislocations in  $L_{12}$  Ni<sub>3</sub>Al [35]. The results of these calculations are encouraging and suggest that the GSF-PN model is a reasonable approximation for planar cores in intermetallic alloys.

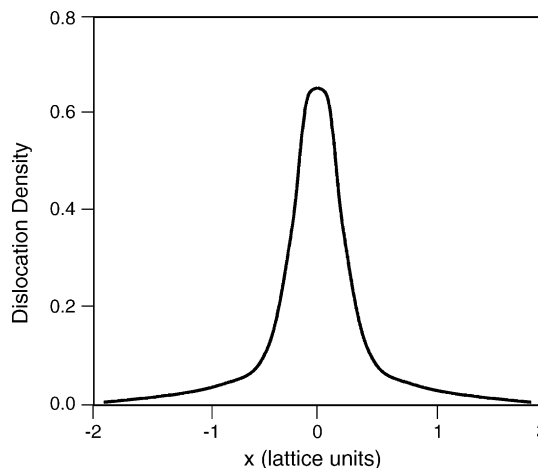


Fig. 10. A schematic of the dislocation density on the  $(1\ 1\ 1)$  plane derived using the GSF-PN model employing a  $\gamma$  surface derived from first-principles simulations [25].

#### 4. Summary

First-principles methods are uniquely suited for describing how changes in chemistry will produce changes in plasticity at the atomic scale. Methods based on dislocation dipoles and the FP-GFBC methods have the advantage of unbiased relaxation of the dislocation strain field near the dislocation core. Also the GFBC method is uniquely suited for estimating the Peierls stress of a straight dislocation at very low temperatures. While significant progress has been made in our ability to model the dislocation core in equilibrium, under an applied stress and for different chemistries more research is required to explore the effects of solid solutions on the dislocation core and the ensuing hardening or softening behavior. The simulation of planar dislocation cores is straightforward using the GSF-PN model and this model has been generalized to non-planar cores by Ngan. The accuracy of such a method for determining the Peierls stress for non-planar cores is open to question. However, in materials where planar dislocation cores are assumed to dominate the deformation behavior the GSF-PN model can be a very useful technique.

#### Acknowledgements

The author acknowledges useful discussions with G. Schoeck, A.H.W. Ngan, A.J. Freeman, O.N. Mryasov, and O.Y. Kontsevoi. Also, we acknowledge the support of the Air Force Research Laboratory, the Air Force Office of Scientific Research under contract F33615-01-C-5214 and a grant of computer time from the US Department of Defense High Performance Computing Modernization Program, at the Aeronautical Systems Center-Major Shared Resource Center, on the SGI and IBM-SP3.



## References

- [1] J.W. Christian, *Metal. Trans. A* 14 (1983) 1237–1256.
- [2] G. Taylor, *Prog. Mater. Sci.* 36 (1992) 29–61.
- [3] J.R.K. Bigger, D.A. McInnes, A.P. Sutton, M.C. Payne, I. Stich, R.D. King-Smith, D.M. Bird, L.J. Clarke, *Phys. Rev. Lett.* 69 (1992) 2224–2227.
- [4] J. Bennetto, R.W. Nunes, D. Vanderbilt, *Phys. Rev. Lett.* 79 (1997) 245–248.
- [5] X. Blase, Karin Lin, A. Canning, S.G. Louie, D.C. Chrzan, *Phys. Rev. Lett.* 84 (2000) 5780–5793.
- [6] W. Cai, V.V. Bulatov, J. Chang, J. Li, S. Yip, *Phys. Rev. Lett.* 86 (2000) 5727–5731.
- [7] S. Ismail-Beigi, T.A. Arias, *Phys. Rev. Lett.* 84 (2000) 1499–1503.
- [8] S.L. Frederiksen, K. Jacobsen, *Phil. Mag.* 83 (2003) 365–375.
- [9] W. Xu, J.A. Moriarty, *Phys. Rev. B* 54 (1996) 6941–6951.
- [10] J.E. Sinclair, P.C. Gehlen, R.G. Hoagland, J.P. Hirth, *J. Appl. Phys.* 49 (1978) 3890–3897.
- [11] S. Rao, C. Hernandez, J. Simmons, T.A. Parthasarathy, C. Woodward, *Phil. Mag. A* 77 (1998) 231–256.
- [12] P. Giannozzi, S. de Gironcoli, P. Pavone, S. Baroni, *Phys. Rev. B* 43 (1991) 7231–7242.
- [13] (a) G. Kresse, J. Hafner, *Phys. Rev. B* 47 (1993) 558–561;  
(b) G. Kresse, J. Hafner, *Phys. Rev. B* 49 (1994) 14251–14269;  
(c) G. Kresse, J. Furthmueller, *Comput. Mater. Sci.* 6 (1996) 15–50.
- [14] C. Woodward, S.I. Rao, *Phys. Rev. Lett.* 88 (2002) 1–4, 216402.
- [15] C. Woodward, S.I. Rao, *Phil. Mag.* 81 (2001) 1305–1316.
- [16] C. Woodward, S.I. Rao, *Phil. Mag.* 84 (2004) 401–413.
- [17] V. Vitek, *Phil. Mag.* 18 (1968) 773–786.
- [18] M. Fahnle, S. Schweitzer, C. Elasser, A. Seeger, in: M. Doyama (Ed.), *International Conference on Computer Applications to Materials Science and Engineering*, North Holland Press, Amsterdam, 1992, p. 864.
- [19] V. Vitek, K. Ito, R. Siegl, S. Znam, *Mater. Sci. Eng. A239–A240* (1997) 752–760.
- [20] N.I. Medvedeva, O.N. Myrasov, Y.N. Gornostyrev, D.L. Nivikov, A.J. Freeman, *Phys. Rev. B* 54 (1996) 13506–13514.
- [21] R. Peierls, *Proc. Phys. Soc., London B* 52 (1940) 34.
- [22] F.R.N. Nabarro, *Proc. Phys. Soc., London B* 59 (1947) 256.
- [23] J.W. Christian, V. Vitek, *Rep. Prog. Phys.* 33 (1970) 307–411.
- [24] G. Schoeck, *Phil. Mag.* 69 (1994) 1085–1095.
- [25] (a) O.N. Myrasov, Y.N. Gornostyrev, A.J. Freeman, *Phys. Rev. B* 58 (1998) 11927–11932;  
(b) O.N. Myrasov, Y.N. Gornostyrev, M. van Schilfgaarde, A.J. Freeman, *Acta Mater.* 50 (2002) 4545–4554.
- [26] A.H.W. Ngan, *J. Mech. Phys. Solids* 45 (1997) 903–921.
- [27] V.V. Bulatov, E. Kaxiras, *Phys. Rev. Lett.* 78 (1997) 4221–4225.
- [28] (a) L. Gang, N. Kioussis, V.V. Bulatov, E. Kaxiras, *Phys. Rev. B* 62 (2000) 3099–3108;  
(b) L. Gang, Q. Zhang, N. Kioussis, E. Kaxiras, *Phys. Rev. Lett.* 87 (2001), 095501-1-4.
- [29] S.I. Rao, C. Woodward, *Phil. Mag.* 81 (2001) 1317–1327.
- [30] M.S. Deusbery, V. Vitek, D. Bowen, *Proc. R. Soc. A* 332 (1973) 85.
- [31] A. Seeger, C. Wuthrich, *Nuovo Cim. B33* (1976) 38.
- [32] M.S. Duesbery, V. Vitek, *Acta Mater.* 46 (1998) 1481–1492.
- [33] F. Louchet, B. Viguier, *Phil. Mag. A* 71 (1995) 1313.
- [34] S. Sriram, D.M. Dimiduk, P.M. Hazzledine, V.K. Vasudevan, *Phil. Mag.* 76 (1997) 965.
- [35] S. Kohlhammer, M. Fahnle, G. Schoeck, *Scripta Mater.* 39 (1998) 359–363.